

A Preliminary Morphology of Precipitation Systems In Tropical Northern Australia

T. KEENAN(*) and R. E. CARBONE(#)

(*)*BMRC PO Box 1289K GPO
Melbourne, Australia 3001*

(#)NCAR¹ PO Box 3000
Boulder CO 80307.3000-U.S.A

1. Introduction.

An observing station has been established in Darwin, north Australia (12°S-131°E) to provide monsoon rainfall data required for the Tropical Rainfall Measuring Mission (TRMM) of the National Aeronautics and Space Administration (NASA) and the Tropical Oceans and Global Atmosphere (TOGA) project.

The Darwin station consists of the National Oceanic and Atmospheric Administration (NOAA)/TOGA Doppler radar, rawinsondes every 12h, wind soundings every 6h, a mesoscale network of 26 tipping bucket raingauges and surface observing network. Details of the Darwin area, the network and observational procedures are given by Keenan et al (1988).

The aim of this paper is to present a preliminary morphology of the precipitation systems that were observed during the 1987-88 summer monsoon period. Climatological characteristics of Darwin are presented together with examples of precipitation systems observed during monsoon and drier transition and break periods. Precipitation systems are also discussed in the general context of the Bulk Richardson number parameter i.e. convective available potential energy (CAPE) and vertical shear of the lower tropospheric winds.

Herein, radar "reflectivity" Z is defined as the sixth moment of the raindrop size distribution. In accordance with standard practice, $\text{dBZ} = 10 \log_{10} Z$ and is expressed in units of $\text{mm}^6 \text{m}^{-3}$. For quasi-equilibrium drop-size distributions:

$$\begin{aligned} 23\text{dBZ} &= 1 \text{ mmh}^{-1} \\ 55\text{dBZ} &= 100 \text{ mmh}^{-1} \text{ (Marshall and Palmer, 1948)} \end{aligned}$$

2. Climatological characteristics of the summer monsoon.

Darwin is situated in the maritime continent region and experiences pronounced wet and dry seasons. The wet season extends from December through March and is characterized by low level equatorial westerly flow with so-called "transition" and "break" periods when there is a low- to mid-level easterly flow. As shown in Fig.1, the 1987-88 break and transition easterly flow had a relatively uniform layer of shear extending to the easterly maximum near 700 mb. While westerly flow is normally encountered in the 400-150 mb level during the break and transition periods, the 1987-88 wet season mean shows weak easterly flow in this layer. During the monsoon westerly

1. NCAR is sponsored by the National Science Foundation



flow, the low level shear is reversed and the surface shear layer is very shallow. Maximum westerly winds occur at 900 mb but extend to 400 mb in a deep layer of westward shear. Easterly flow was apparent above 400mb during the monsoon westerly flow.

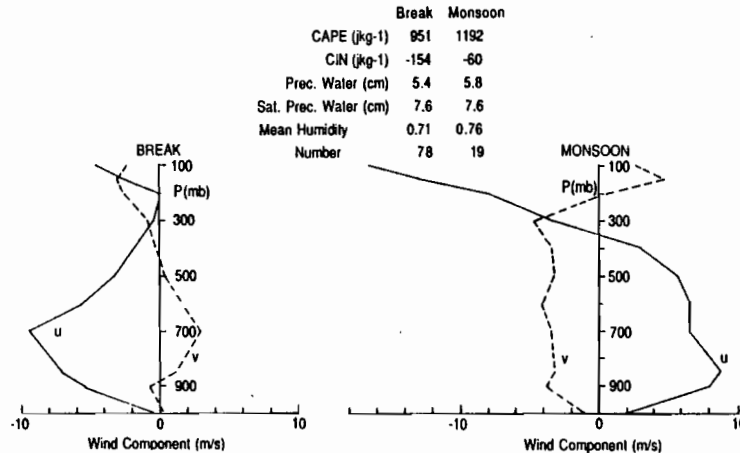


FIG.1. Mean vertical structure of 1987-88 break and monsoon period flow at Darwin.

The CAPE (Moncrieff and Green, 1972) is comparable during both the break and monsoon periods although the Convective Inhibition (CIN), as defined by Colby (1983) is slightly larger for the former. The mean precipitable water content for the two regimes are large and typical of tropical situations. In comparison, they are at least twice the size of values found in the Oklahoma data of Bluestein and Parks (1983).

The preceding climatological data gives the mean characteristics of the monsoon and break season flow. The aim will now be to present some examples of convective systems and to relate the occurrence of the systems to specific dynamic regimes. The examples have been selected to highlight the population of systems encountered at Darwin and to elucidate some features relevant to convective structure and propagation mechanisms.

3. Monsoon flow systems.

Figure 2 illustrates a typical monsoon condition with widespread coastal and oceanic precipitation containing relatively disorganized and weak convection. The RHI in the direction of 270° reveals echo tops between 10 and 14 km with very weak horizontal reflectivity and vertical shear of the horizontal wind above the 0°C melting level near 5 km. The most vigorous convection appears to be within 10 km of the radar where low-level reflectivity gradients are strongest and echo tops are highest. Radial velocities confirm westerly flow below 5 km and easterly flow above. Patches of westerly momentum above 5 km are likely the result of convective momentum transport. CAPE of 450 J kg^{-1} is relatively small and low-level shear² of $1.9 \times 10^{-3} \text{ s}^{-1}$ is weak. The region of precipitation is quasi-stationary throughout the event.

Figure 3 depicts another monsoon situation showing embedded convection organized in patches and short line-segments. The reflectivity exceeds 50 dBZ in the more intense convective cores. The echoes are quasi-stationary but there is some

2. Unless otherwise stated the shear has been taken over the lowest 3km in this paper.

tendency for slow southward movement with a gradual trend toward more linear organization in the convective areas. Soundings reveal CAPE of 1700 Jkg^{-1} and low-level shear is $3.3 \times 10^{-3} \text{ s}^{-1}$.

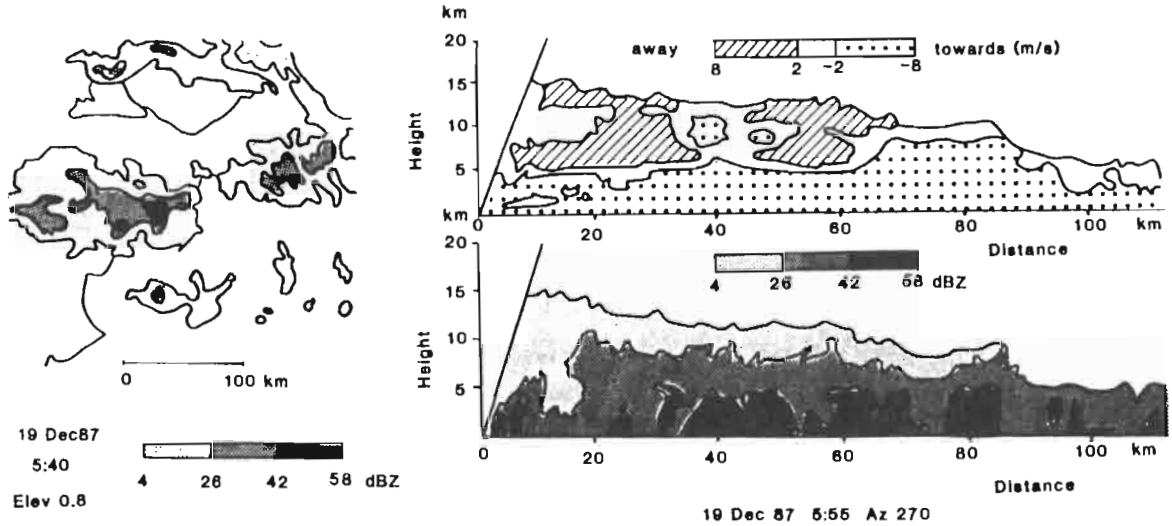


FIG.2. Radar reflectivity of a monsoon band observed at Darwin. PPI structure (a) and RHI reflectivity and radial velocity (b). RHI reflectivity (c).

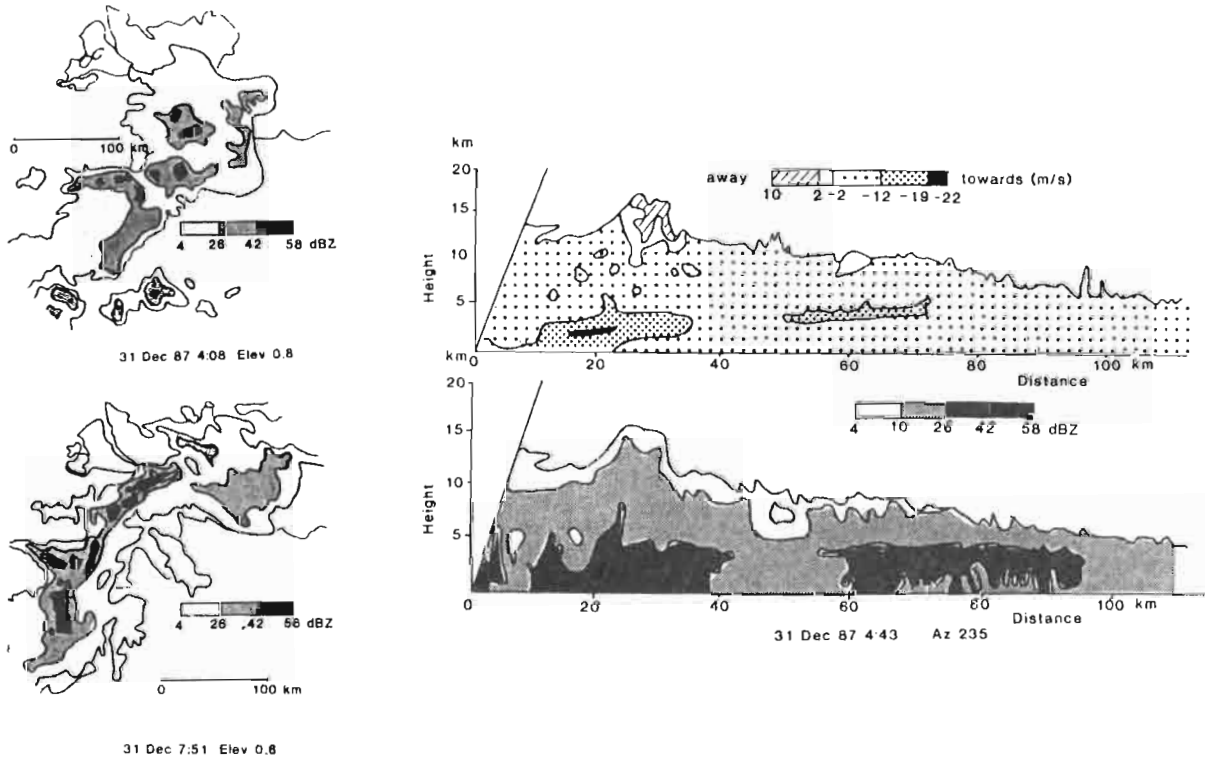


FIG.3 Evolution of the horizontal reflectivity structure of a monsoonal band (a) and (c) and RHI cross-section of reflectivity and radial velocity (b).

The entire system is embedded in westerly flow throughout the 10 km depth of precipitation echo as evidenced in Fig.3b which is an RHI along 235° azimuth. The scan plane passes through two major convective line segments and trailing stratiform precipitation. The melting level is evident from increased reflectivity near 5 km and the depth of convection is seen to range from 10 to 15 km in the near and far bands, respectively. Doppler velocity structure reveals downward transport of southwesterly momentum descending from the 4 km level at 70 km range to less than 2 km at 12 km range underneath the convective bands. This low-level westerly jet structure is part of the strong confluence field at the base of deep convection. By inference from reflectivity and velocity structures, we conclude that updrafts are tilted 30° to 40° (from zenith) toward the southwest in a downshear direction (above 3 km). This organization is reminiscent of classical tropical squall lines as depicted by Houze (1977).

Figure 3c illustrates a much higher degree of organization at 0750 LST where a major convective line is evident. The precipitation region has reversed motion to a northerly direction such that the major band is now located off-shore. Lower amplitude, periodic transverse structure is also evident with 20-50 km spacing. This degree of convective organization is often not evident in monsoon situations.

4. Break and transition season systems.

a. Continental Convection.

Continental convection, is observed regularly during the afternoon and evening periods of the break and transition season. The characteristic evolution consists of scattered isolated cells later aggregating and often forming weak squall lines. Such structure is depicted in Fig.4. Typically, as shown in Fig. 4b the cells are vertically erect and deep with tops above 15 km. Continental cells form under a wide range of conditions. For this example, the CAPE was 920 J kg^{-1} and the low level shear was $2.9 \times 10^{-3} \text{ s}^{-1}$.

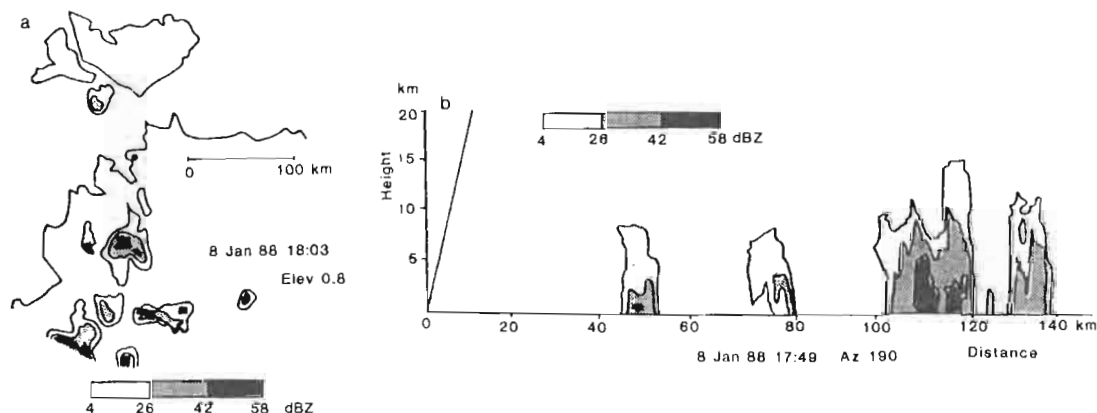


FIG.4. PPI (a) and RHI (b) of continental convection observed with the Darwin radar.

b. Maritime Continent Thunderstorms.

Thunderstorms characteristic of the maritime continent are observed on 65% of days over the islands to the north of Darwin during the transition and break seasons. These storms can exhibit a variety of forms including both single and multiple cell storm. A multicellular type is shown in Fig.5. As shown in the RHI of Fig 5b, the major cells are vertically erect reaching up to 17-18km with a simple low level convergent and upper level divergent structure. CAPE and low level shear values representative of the

pre-storm environment in Fig.5 are 1620 J kg^{-1} and $1.6 \times 10^{-3} \text{ s}^{-1}$ respectively. The Island Thunderstorm Experiment, described by Keenan et al (1989) was undertaken during November and December 1988 to obtain experimental data on these systems. The tilted column of receding Doppler velocity reveals the upward transport of boundary layer momentum in the main updraft. The updraft is tilted 40° from zenith.

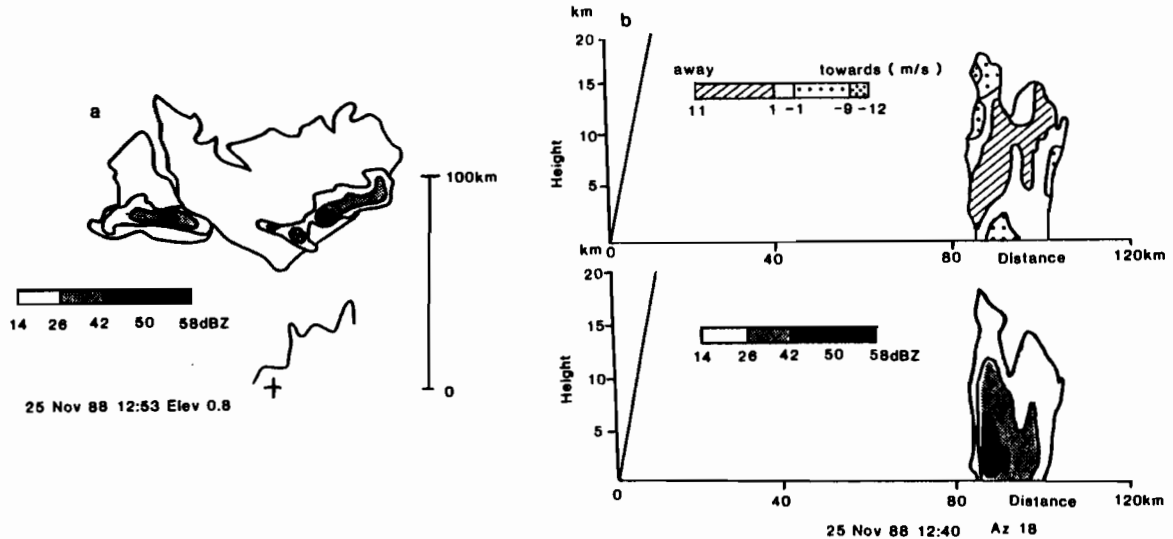


FIG.5. PPI (a) and RHI (b) of reflectivity and radial velocity of an island thunderstorm observed with the Darwin radar.

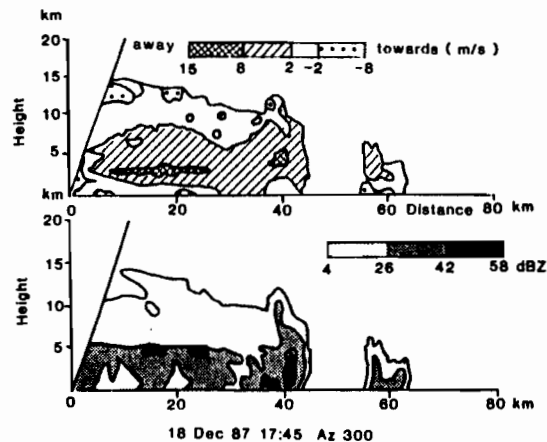


FIG.6. Darwin radar RHI of reflectivity and Doppler derived radial velocity through a "classical" tropical squall line.

c. Squall lines.

Figure 6 is an RHI perpendicular to a classical tropical squall line very similar to those reported from the Global Atmosphere Research Program Atlantic Tropical Experiment (GATE) by Houze (1977), Zipser and LeMone (1980), Barnes and Sieckman (1984) among others. Such squall lines are noted for continual development of new cells along the leading edge of the convective line; a rear-to-front, descending mid-level inflow jet; and pronounced trailing stratiform precipitation. Often there is a precipitation "trough" between the rear flank of the convective line and the stratiform area. In Fig. 6, these features are evident in the reflectivity and Doppler velocity fields. CAPE is 920 J kg^{-1} and low-level shear is $1.1 \times 10^{-3} \text{ s}^{-1}$. These conditions are very similar to those

experienced in GATE (Barnes and Sieckman, 1984). Of special interest is the wave-like pattern in Doppler velocity behind the convective line. The pattern is suggestive of a 20-30 km gravity wave where the first depression (at 28 km) is coincident with the rear flank "trough". Increased vertical shear and vertical mixing is also suggested by the echo top pattern at 15 km range and 10 km height. The rear (easterly) inflow jet is located at 3 km height and has a magnitude of 10 m s^{-1} . The undisturbed environmental flow at 3 km was 5 m s^{-1} , the same speed as the squall line movement.

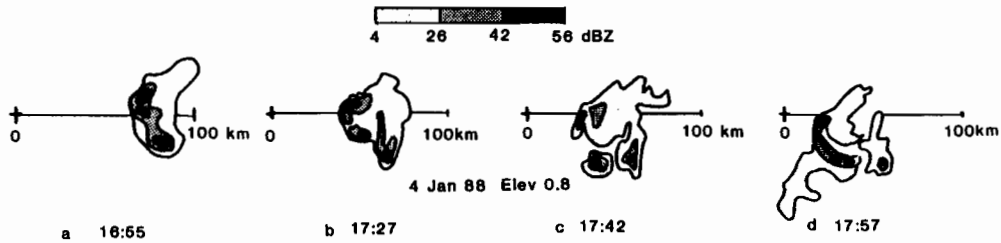


FIG.7. Darwin radar reflectivity time sequence for a squall line exhibiting discontinuous propagation.

Figures 7 show a time sequence of squall line evolutions on 4 January 1988. We distinguish this situation from that shown in Fig.6 because propagation is clearly discontinuous. Close examination of Figs 7a-d reveals a succession of three small convective lines which initiate 10-30 km ahead of the previous line. While direct thermodynamic evidence is not available, Doppler velocities at low levels behind each convective line suggest that a rapidly forward-spreading cold pool is responsible in each instance. While each individual convective line translates from $7\text{-}10 \text{ m s}^{-1}$, the aggregate convective system propagates at 16.5 m s^{-1} eastward. This rate of propagation exceeds the environmental easterly winds at any level (12 m s^{-1} maximum). Only a shallow planetary boundary layer cold pool transports mass at a rate which equals or exceeds the aggregate propagation rate. Conditions in this case have $\text{CAPE}=618 \text{ J kg}^{-1}$ and low-level shear of $3.9 \times 10^{-3} \text{ s}^{-1}$.

Figures 8 show the squall line of 13 January which exhibits characteristics similar to mid-latitude systems. The plan view of reflectivity (a) shows slight bowing in the shape of a vigorous convective line together with a weak trailing precipitation region. Reflectivity and velocity RHI's, along azimuth 68° , reveal a well-developed leading anvil and an updraft which is tilted rearward $\sim 55^\circ$ from zenith. This is a consequence of unusually deep and strong easterlies aloft which exceed the squall line translation speed by roughly 5 m s^{-1} . Convective cells develop continually at the leading edge as predicted by the theory of Rotunno et al (1988). An advancing surface cold pool is implied by very strong approaching Doppler velocities near the surface in the heavy precipitation cores. Intense vertical shear of the horizontal wind is evident at 43 km range, between 1.5 and 2 km, where shear exceeds $2 \times 10^{-2} \text{ s}^{-1}$. CAPE is quite large, at 2050 J kg^{-1} , a value comparable to that found in mid-latitudes. Environmental low-level shear is moderate at $4.2 \times 10^{-3} \text{ s}^{-1}$. Convective line movement is toward the west at 12.5 m s^{-1} . This speed is faster than low to mid-tropospheric easterlies and slower than easterly momentum generated by the hypothesized spreading cold pool.

Figure 9. shows an RHI of a squall system with a relatively large CAPE of 2100 J kg^{-1} and low-level shear of $3.2 \times 10^{-3} \text{ s}^{-1}$. The RHI is at 68° azimuth and shows a stratiform region ahead of the westward-moving squall line. The stratiform region is, in fact, the product of a preceding squall line with the new convective line overtaking it from the rear. Note the elevated reflectivity maximum between 5 and 9 km height, the rear flank weak echo vault between 9 and 14 km height and the strong, mid-tropospheric convergence several kilometres below. The depth of convection extends to nearly 20 km.

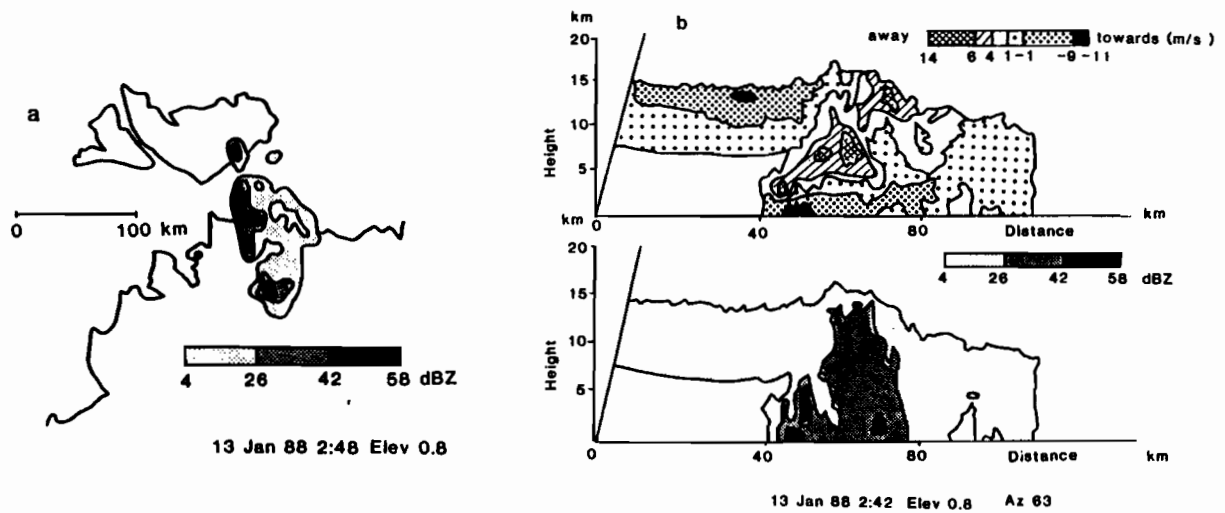


FIG.8. Darwin PPI (a) and RHI (b) observed reflectivity and radial velocity for a squall line exhibiting the characteristics of a mid-latitude system.

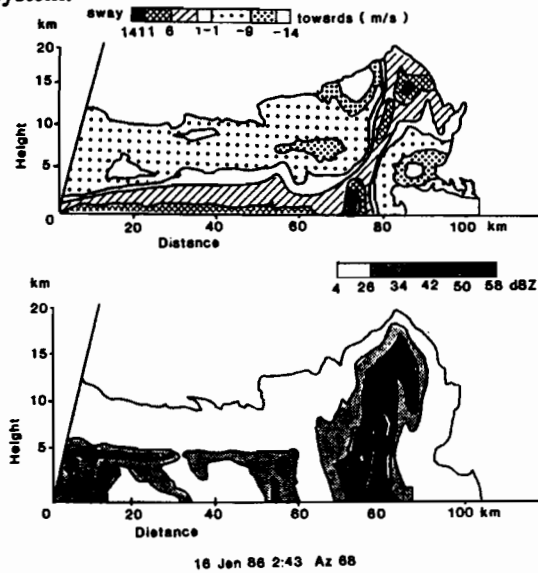


FIG.9. RHI of reflectivity and radial velocity for a very intense tropical squall observed at Darwin.

Clearly there are a diversity of squall line structures in the Darwin area which sometimes differ markedly from tropical squall organizations observed in the GATE area and in Africa.

5. Convective organization and mesoscale environment.

The aim of this section is to consolidate some ideas by examining the relationship of convective organizations observed near Darwin with the variety of convective systems observed elsewhere. In addition, some concepts relevant to squall line motion will be discussed.

a. Bulk Richardson number depiction.

A convenient method of classifying the spectrum of convective systems is through the CAPE and kinetic energy associated with the vertical shear of the flow e.g. Moncrieff and Miller (1976), Weisman and Klemp (1982) and Rasmussen and

Wilhelmson (1983), Carbone et al. (1989), Ray (1989). Such a classification provides a basis for incorporating the roles played by buoyant energy of the storm and that of the environmental kinetic energy with which the storm interacts.

A depiction of storm types based on the above principle is summarized in Fig. 10 using low level shear and CAPE in the manner of Rasmussen and Wilhelmson (1983). In the context of this paper, low level shear is taken to be representative of the depth of the naturally occurring shear layer. Thus various levels have been used to calculate the low level shear but all range over the lowest 20-35% of the depth of convection. e.g. for hurricane and cold frontal rainband data we employ shear layers 1-2km deep; for Darwin, we use the 0-3km shear; data taken from Rasmussen and Wilhelmson (1983) use the 0-4 km. Shear magnitude is calculated for the component perpendicular to linear convective lines where applicable.

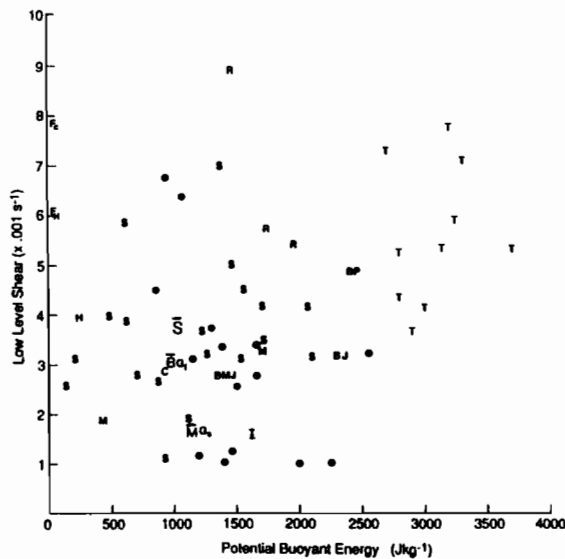


FIG.10. Storm occurrence as a function of buoyant energy and low level shear. See text for a description.

The data presented in Fig.10 are based on the following:

1. Tornadoic storms (T), non-tornadoic storms with a mesocyclone (R), and various other North American storms (●) as given by Rasmussen and Wilhelmson (1983);
2. Darwin systems-Squall lines (S), Monsoon systems (M), the example of Continental convection (C), the example of an island thunderstorms (I), the mean of the squall systems (B) and as per Fig.1 the Monsoon Mean (M "bar") and the Break Mean (B "bar");
3. GATE fast (G_f) and Slow (G_s) moving squalls as given by Barnes and Sieckman (1984);
4. Mean values representative of hurricane rainbands using values given by Barnes et al (1983), Barnes and Stossmeister (1986);
5. Frontal rainbands as presented by Carbone (1982), Hobbs and Persson (1982)
6. Non-severe squall lines (BMJ) of Bluestein et al (1987), severe squall lines (BJ) of Bluestein and Jain (1985), and isolated super cell storms (BP) of Bluestein and Parks (1983).

The most significant feature evident in Fig.10 is the considerable range of buoyant energy and wind shear over which Darwin storms extend. They range from the expected tropical range of relatively low shear and buoyant energy to that expected from

midlatitude severe storms. The centroid of the Darwin squall cluster is somewhat less than the mean representative of the environment of North American plains type non-severe squall lines of Bluestein et al (1987). The dynamic range of the spectrum of systems encompasses that of the Oklahoma severe squall lines presented by Bluestein and Jain (1985). This edge of the tropical convective activity includes the likelihood of systems exhibiting mesoscale cyclonic rotation and possibly even tornadic storms. That such phenomena could occur or be postulated to occur from such a small sample of cases is surprising but is supported from Bureau of Meteorology reports of tornadic damage on occasions in the Darwin area.

The so-called "typical" tropical squall line i.e. the line most similar to that discussed by Houze (1977) appears somewhat dissimilar to many of the examples presented herein. The location of this storm in Fig.10 is toward the low shear extreme of Darwin conditions at 9201.1×10^{-3} .

As Darwin is affected by tropical cyclones, it would be expected that that low buoyant energy/average shear range of hurricane rainbands shown in Fig.10 would also be experienced in Darwin. Only the very high shear/low buoyancy regions of frontal rainbands and high shear extreme buoyancy regimes are not represented in the Darwin cases examined.

The monsoon systems also demonstrate a significant range of possible modes. The data presented here show that monsoon systems appear to be best characterized by differences in CAPE values. The case in Fig.3 had a CAPE of 1700 J kg^{-1} and represents a departure from the almost moist-adiabatic profile expected for monsoon conditions. It also contained various convective line structures both in the early and late stages of its lifetime. During these periods, the planetary boundary layer shear was as strong as $5 \times 10^{-3} \text{ s}^{-1}$.

The relationship of Darwin data to those of the much examined GATE systems raises questions about representing the tropics. The GATE fast movers of Barnes and Sieckman (1984) are on the lower buoyancy and lower shear side of the tropical squall spectrum. The GATE slow movers appear to occur in conditions similar to the Darwin monsoon systems. That differences exist between mean GATE population and those observed herein has important implications in the use of GATE derived vertical convective heating profiles. The observed differences in the dynamical characteristics of the convective systems implies both larger amplitude heating and higher heating in the troposphere than in the GATE region. Recent results from the Australian Monsoon Experiment of Frank and McBride (1989) offer support that the vertical profile of convective heating in the Australian region is indeed different from GATE. Conversely many similarities may be noted to West African tropical squall systems as examined by Roux (1988).

b. Propagation.

Some lines of the Darwin squalls translate at or near the speed of the environmental winds and others move faster. The latter indicate some form of convective system propagation. The kinematic evidence suggests that cold pool spreading is a common mechanism, but this hypothesis requires confirmation from thermodynamic data. Such a convective-scale mass transportive process seems to be very important. The rate of spreading of the cold domes appears to be prevalent in these examples, given strong rear-to-front flow near the surface immediately behind the convective line.

Continuous propagation is observed in most of the squall systems including the mid-latitude analogy of Fig.8. The convective lines of cells moved faster than the environmental wind at any level although cell motions were less than the rate of expansion of the cold pool. Discontinuous propagation was also evident where the

aggregate system propagated faster than the individual line motion and faster than any environmental flow. Individual convective lines moved slower than the maximum low level environmental winds.

6. Relationship to the TOGA COARE western Pacific warm pool.

The relationship of mesoscale precipitation systems near Darwin to those which occur over the TOGA COARE Western Pacific Warm Pool (WPWP) is unclear. As this study has demonstrated, a large variety of modes of convection can exist within one area. In addition, as the worldwide comparison with GATE has indicated a convective regime in one area may not be representative of that found elsewhere. As a result, major differences can exist in the vertical profile of heating as found by Frank and McBride (1989) for the GATE, Western Pacific and AMEX regions.

Darwin observations are subject to jet-like easterly flow during break and transition season flow. This is in contrast to weaker, deep easterly flow anticipated over WPWP. However, westerly bursts over the the equatorial warm pool are likely to be shallow if they are related to Boreal winter synoptic disturbances. The combination of shallow, westerly bursts with overlying easterlies could provide a low-level shear similar to that experienced in Darwin during break periods. The WPWP region also experiences a period of monsoonal westerly type flow over the southern hemisphere during the northern winter (Atkinson, 1971). The possibility of a similarity with Darwin monsoon type systems therefore exists at that time. If so, then Darwin data may be a good proxy dataset for the mesoscale structure of convective systems within WPWP.

Bulk Richardson number considerations alone, however, are insufficient to establish the relationship between the propagation of mesoscale convective systems (MCS) and the WPWP. Near Darwin, evidence exists for spreading cold pools being the dominant planetary boundary layer (PBL) mechanism for MCS maintenance and propagation. This mechanism is very dependent both on the PBL hydrodynamic stability and the overlying relative humidity structure where evaporation and melting of hydrometeors generate the spreading cold pool. Conditions over TOGA COARE may not be favourable for cold pool production and maintenance, thus invalidating this propagation and maintenance mechanism. The underlying oceanic surface may act to destroy the cold pool more quickly than over continental regions. Stability in the oceanic PBL may be more conducive to the excitation of trapped gravity waves as the dominant propagation mechanism.

Such potential differences have far-reaching consequences to the phase relationship between the WPWP and the location of mature MCS's. Furthermore, these differences markedly alter the surface wind stress experienced at the interface surface since cold pools are mass-transportive whereas gravity waves are essentially energy-transportive. As a consequence of such uncertainties, it is not possible to project whether convective lines will lead or lag eastward-migration of the warm pool.

The foregoing indicates a need to gather a comprehensive microscale and mesoscale data set on storms within the WPWP region. An intensive wind profiler and thermodynamic sounding network together with Doppler radar and research aircraft observations could assist to resolve the many uncertainties.

7. Summary.

Using a limited sample of convective storms observed during the summer monsoon at Darwin during 1987-88 it has become apparent that a surprisingly wide range of convective modes can exist in a tropical environment. The applicability of these

modes of convective activity to the mesoscale structure of the TOGA COARE region is largely unknown and requires investigation before fundamental questions on the relationship between the convection and the TOGA COARE warm pool is understood.

Acknowledgments. The authors wish to thank Dr Joanne Simpson, NASA Goddard Space Flight Center, Dr. J. Michael Hall of NOAA, Office of Climate and Atmospheric Research and Dr M. Manton of the BMRC, Australia for their continued support of this project.

REFERENCES

- Atkinson, G.D., 1971: Forecasters guide to tropical meteorology. *Tech. Rept. 240 Air Weather Service (MAC) US AirForce*, 360 p.
- Barnes, G.M., E.J. Zipser, D.P. Jorgensen and F.D. Marks, 1983: Mesoscale and Convective Scale Structure of a Hurricane Rainband. *J. Atmos. Sci.*, **40**, 2125-2137.
- Barnes, G.M., and K.Sieckman, 1984: The Environment of Fast-and- Slow-Moving Tropical Mesoscale Convective Cloud Lines. *Mon. Wea. Rev.*, **112**, 1782-1794.
- Barnes, G.J., and G.J. Stossmeister, 1986: The Structure and Decay of a Rainband in Hurricane Irene (1981). *Mon. Wea. Rev.*, **114**, 2590-2601.
- Bluestein, H.B., and C.R. Parks, 1983: A Synoptic and Photographic Climatology of Low-Precipitation Severe Thunderstorms in the Southern Plains. *Mon. Wea. Rev.*, **111**, 2034-2046.
- Bluestein, H.B., and M.H. Jain, 1985: Formation of Mesoscale Lines of Precipitation: Severe Squall Lines in Oklahoma during the Spring. *J. Atmos. Sci.*, **42**, 1711-1732.
- Bluestein, H.B., G.T. Marx and M.H.Jain, 1987: Formation of Mesoscale Lines of Precipitation: Nonsevere Squall Lines in Oklahoma during the Spring. *Mon. Wea. Rev.*, **115**, 2719-2727.
- Carbone, R.E., 1982: A Severe Frontal Rainband Part I: Stormwide Hydrodynamic Structure. *J. Atmos. Sci.*, **39**, 258-279.
- Carbone, R., B. Foote, M. Moncrieff, T. Gal-Chen, W. Cotton, M. Hjelfelt, F. Roux, G. Heymsfield, E. Brandes, 1989: *Radar in Meteorology*, Chapter 26b, Panel Report on Convective Dynamics, Amer. Meteor. Soc., Boston, Mass., Ed. D. Atlas (In press)
- Colby, F.P. Jr., 1983: Convective inhibition as a predictor of the outbreak convection in AVE-SESAME II. *Preprints, 13th Conf. on Severe Local Storms*, Tulsa, Amer. Meteor. Soc., 324-327.
- Frank, W.M. and J.L.McBride, 1989: Vertical Profiles of the Convective Heat Source in AMEX: A Comparison with GATE. Submitted to *Mon. Wea. Rev.*
- Hobbs, P.V., and P.Ola G. Persson, 1982: The Mesoscale and Microscale Structure and Organization of Clouds and Precipitation in Midlatitude Cyclones. Part V: The Substructure of Narrow Cold- Frontal Rainbands. *J. Atmos. Sci.*, **39**, 280-295.
- Houze, R.A., Jr., 1977: Structure and Dynamics of a Tropical Squall-line System. *Mon. Wea. Rev.*, **105**, 1540-1567.
- Keenan, T.D., G.J. Holland, M.J.Manton and J.Simpson, 1988: TRMM Ground Truth in a Monsoon Environment: Darwin, Australia. *Aust. Meteor. Mag.*, **36**, 91-90.
- Keenan, T.D., B.R. Morton, M.J. Manton and G.J. Holland, 1989: The Island Thunderstorm Experiment (ITEX)-A Study of Tropical Thunderstorms in the Maritime Continent. *Bull. Amer. Meteor. Soc.*, **70**, 152-159.
- Marshall, J.S. and W.M. Palmer, 1948: The distribution of raindrops with size. *J. Meteor.*, **5**, 165-166.

- Moncrieff, M.W. and J.S.A. Green, 1972: The propagation and transfer properties of steady convective overturning in shear. *Quart. J. Roy. Meteor. Soc.*, **98**, 336-352.
- Moncrieff, M.W., and M.J Miller, 1976: The dynamics and simulation of tropical cumulonimbus and squall lines. *Quart. J. Roy. Meteor. Soc.*, **102**, 373-394.
- Rasmussen, E.N. and R.B. Wilhelmson, 1983: Relationships between Storm Characteristics and 1200 GMT Hodograph, Low Level Shear and Stability. Preprints, *13th Conference on Severe Local Storms*, Tulsa, Ok, Amer. Meteor. soc., Boston, 55-58.
- Ray, P.S. 1989: *Radar in Meteorology*, Chapt. 26a, Convective Dynamics, Amer. Meteor. Soc., MA, Ed. D. Atlas (In press).
- Roux F., 1988: The West African Squall Line Observed on 23 June 1981 during COPT 81: Kinematics and Thermodynamics of the Convective Region. *J. Atmos. Sci.*, **45**, 406-426.
- Weisman, M.L., and J.B. Klemp. 1982: The Dependence of Numerically Simulated Convective Storms on Vertical Wind Shear and Buoyancy. *Mon. Wea. Rev.*, **110**, 504-520.
- Weisman, M.L., and J.B. Klemp. 1986: Characteristics of Isolated Convective Storms, Chapt. 15, *Mesoscale Meteorology and Forecasting*, Amer. Meteor. Soc., Ed. P. Ray, 793 p.
- Zipser, E.J., and M.A. LeMone, 1980: Cumulonimbus Vertical Velocity Events in GATE. Part II: Synthesis and Model Core Structure. *J. Atmos. Sci.*, **37**, 2458-2469.

**WESTERN PACIFIC INTERNATIONAL MEETING
AND WORKSHOP ON TOGA COARE**

**Nouméa, New Caledonia
May 24-30, 1989**

PROCEEDINGS

edited by

Joël Picaut *
Roger Lukas **
Thierry Delcroix *

* ORSTOM, Nouméa, New Caledonia
** JIMAR, University of Hawaii, U.S.A.

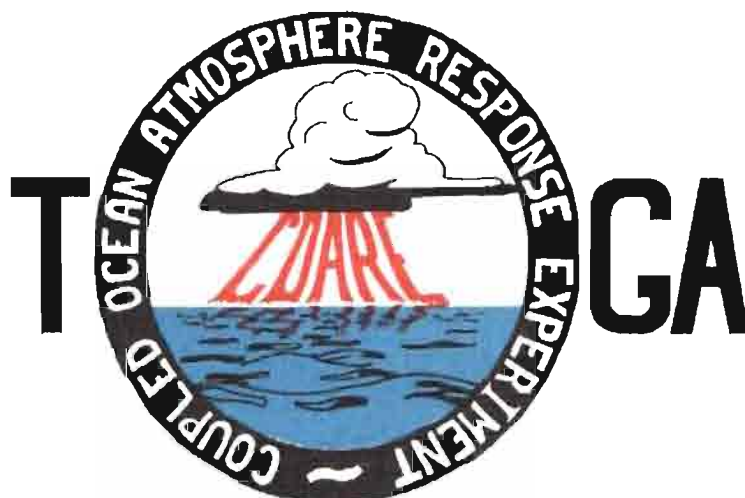


TABLE OF CONTENTS

ABSTRACT	i
RESUME	iii
ACKNOWLEDGMENTS	vi
INTRODUCTION	
1. Motivation	1
2. Structure	2
LIST OF PARTICIPANTS	5
AGENDA	7
WORKSHOP REPORT	
1. Introduction	19
2. Working group discussions, recommendations, and plans	20
a. Air-Sea Fluxes and Boundary Layer Processes	20
b. Regional Scale Atmospheric Circulation and Waves	24
c. Regional Scale Oceanic Circulation and Waves	30
3. Related programs	35
a. NASA Ocean Processes and Satellite Missions	35
b. Tropical Rainfall Measuring Mission	37
c. Typhoon Motion Program	39
d. World Ocean Circulation Experiment	39
4. Presentations on related technology	40
5. National reports	40
6. Meeting of the International Ad Hoc Committee on TOGA COARE	40
APPENDIX: WORKSHOP RELATED PAPERS	
Robert A. Weller and David S. Hosom: Improved Meteorological Measurements from Buoys and Ships for the World Ocean Circulation Experiment	45
Peter H. Hildebrand: Flux Measurement using Aircraft and Radars	57
Walter F. Dabberdt, Hale Cole, K. Gage, W. Ecklund and W.L. Smith: Determination of Boundary-Layer Fluxes with an Integrated Sounding System	81

MEETING COLLECTED PAPERS

WATER MASSES, SEA SURFACE TOPOGRAPHY, AND CIRCULATION

Klaus Wyrtki: Some Thoughts about the West Pacific Warm Pool	99
Jean René Donguy, Gary Meyers, and Eric Lindstrom: Comparison of the Results of two West Pacific Oceanographic Expeditions FOC (1971) and WEPOCS (1985-86)	111
Dunxin Hu, and Maochang Cui: The Western Boundary Current in the Far Western Pacific Ocean	123
Peter Hacker, Eric Firing, Roger Lukas, Philipp L. Richardson, and Curtis A. Collins: Observations of the Low-latitude Western Boundary Circulation in the Pacific during WEPOCS III	135
Stephen P. Murray, John Kindle, Dharma Arief, and Harley Hurlburt: Comparison of Observations and Numerical Model Results in the Indonesian Throughflow Region	145
Christian Henin: Thermohaline Structure Variability along 165°E in the Western Tropical Pacific Ocean (January 1984 - January 1989)	155
David J. Webb, and Brian A. King: Preliminary Results from Charles Darwin Cruise 34A in the Western Equatorial Pacific	165
Warren B. White, Nicholas Graham, and Chang-Kou Tai: Reflection of Annual Rossby Waves at The Maritime Western Boundary of the Tropical Pacific	173
William S. Kessler: Observations of Long Rossby Waves in the Northern Tropical Pacific	185
Eric Firing, and Jiang Songnian: Variable Currents in the Western Pacific Measured During the US/PRC Bilateral Air-Sea Interaction Program and WEPOCS	205
John S. Godfrey, and A. Weaver: Why are there Such Strong Steric Height Gradients off Western Australia ?	215
John M. Toole, R.C. Millard, Z. Wang, and S. Pu: Observations of the Pacific North Equatorial Current Bifurcation at the Philippine Coast	223

EL NINO/SOUTHERN OSCILLATION 1986-87

Gary Meyers, Rick Bailey, Eric Lindstrom, and Helen Phillips: Air/Sea Interaction in the Western Tropical Pacific Ocean during 1982/83 and 1986/87	229
Laury Miller, and Robert Cheney: GEOSAT Observations of Sea Level in the Tropical Pacific and Indian Oceans during the 1986-87 El Nino Event	247
Thierry Delcroix, Gérard Eldin, and Joël Picaut: GEOSAT Sea Level Anomalies in the Western Equatorial Pacific during the 1986-87 El Nino, Elucidated as Equatorial Kelvin and Rossby Waves	259
Gérard Eldin, and Thierry Delcroix: Vertical Thermal Structure Variability along 165°E during the 1986-87 ENSO Event	269
Michael J. McPhaden: On the Relationship between Winds and Upper Ocean Temperature Variability in the Western Equatorial Pacific	283

John S. Godfrey, K. Ridgway, Gary Meyers, and Rick Bailey: Sea Level and Thermal Response to the 1986-87 ENSO Event in the Far Western Pacific	291
Joël Picaut, Bruno Camusat, Thierry Delcroix, Michael J. McPhaden, and Antonio J. Busalacchi: Surface Equatorial Flow Anomalies in the Pacific Ocean during the 1986-87 ENSO using GEOSAT Altimeter Data	301

THEORETICAL AND MODELING STUDIES OF ENSO AND RELATED PROCESSES

Julian P. McCreary, Jr.: An Overview of Coupled Ocean-Atmosphere Models of El Nino and the Southern Oscillation	313
Kensuke Takeuchi: On Warm Rossby Waves and their Relations to ENSO Events	329
Yves du Penhoat, and Mark A. Cane: Effect of Low Latitude Western Boundary Gaps on the Reflection of Equatorial Motions	335
Harley Hurlburt, John Kindle, E. Joseph Metzger, and Alan Wallcraft: Results from a Global Ocean Model in the Western Tropical Pacific	343
John C. Kindle, Harley E. Hurlburt, and E. Joseph Metzger: On the Seasonal and Interannual Variability of the Pacific to Indian Ocean Throughflow	355
Antonio J. Busalacchi, Michael J. McPhaden, Joël Picaut, and Scott Springer: Uncertainties in Tropical Pacific Ocean Simulations: The Seasonal and Interannual Sea Level Response to Three Analyses of the Surface Wind Field	367
Stephen E. Zebiak: Intraseasonal Variability - A Critical Component of ENSO ?	379
Akimasa Sumi: Behavior of Convective Activity over the "Jovian-type" Aqua-Planet Experiments	389
Ka-Ming Lau: Dynamics of Multi-Scale Interactions Relevant to ENSO	397
Pecheng C. Chu and Roland W. Garwood, Jr.: Hydrological Effects on the Air-Ocean Coupled System	407
Sam F. Iacobellis, and Richard C.J. Somerville: A one Dimensional Coupled Air-Sea Model for Diagnostic Studies during TOGA-COARE	419
Allan J. Clarke: On the Reflection and Transmission of Low Frequency Energy at the Irregular Western Pacific Ocean Boundary - a Preliminary Report	423
Roland W. Garwood, Jr., Pecheng C. Chu, Peter Muller, and Niklas Schneider: Equatorial Entrainment Zone : the Diurnal Cycle	435
Peter R. Gent: A New Ocean GCM for Tropical Ocean and ENSO Studies	445
Wasito Hadi, and Nuraini: The Steady State Response of Indonesian Sea to a Steady Wind Field	451
Pedro Ripa: Instability Conditions and Energetics in the Equatorial Pacific	457
Lewis M. Rothstein: Mixed Layer Modelling in the Western Equatorial Pacific Ocean	465
Neville R. Smith: An Oceanic Subsurface Thermal Analysis Scheme with Objective Quality Control	475
Duane E. Stevens, Qi Hu, Graeme Stephens, and David Randall: The hydrological Cycle of the Intraseasonal Oscillation	485
Peter J. Webster, Hai-Ru Chang, and Chidong Zhang: Transmission Characteristics of the Dynamic Response to Episodic Forcing in the Warm Pool Regions of the Tropical Oceans	493

MOMENTUM, HEAT, AND MOISTURE FLUXES BETWEEN ATMOSPHERE AND OCEAN

W. Timothy Liu: An Overview of Bulk Parametrization and Remote Sensing of Latent Heat Flux in the Tropical Ocean	513
E. Frank Bradley, Peter A. Coppin, and John S. Godfrey: Measurements of Heat and Moisture Fluxes from the Western Tropical Pacific Ocean	523
Richard W. Reynolds, and Ants Leetmaa: Evaluation of NMC's Operational Surface Fluxes in the Tropical Pacific	535
Stanley P. Hayes, Michael J. McPhaden, John M. Wallace, and Joël Picaut: The Influence of Sea-Surface Temperature on Surface Wind in the Equatorial Pacific Ocean	543
T.D. Keenan, and Richard E. Carbone: A Preliminary Morphology of Precipitation Systems In Tropical Northern Australia	549
Phillip A. Arkin: Estimation of Large-Scale Oceanic Rainfall for TOGA	561
Catherine Gautier, and Robert Frouin: Surface Radiation Processes in the Tropical Pacific	571
Thierry Delcroix, and Christian Henin: Mechanisms of Subsurface Thermal Structure and Sea Surface Thermo-Haline Variabilities in the South Western Tropical Pacific during 1979-85 - A Preliminary Report	581
Greg. J. Holland, T.D. Keenan, and M.J. Manton: Observations from the Maritime Continent : Darwin, Australia	591
Roger Lukas: Observations of Air-Sea Interactions in the Western Pacific Warm Pool during WEPOCS	599
M. Nunez, and K. Michael: Satellite Derivation of Ocean-Atmosphere Heat Fluxes in a Tropical Environment	611

EMPIRICAL STUDIES OF ENSO AND SHORT-TERM CLIMATE VARIABILITY

Klaus M. Weickmann: Convection and Circulation Anomalies over the Oceanic Warm Pool during 1981-1982	623
Claire Perigaud: Instability Waves in the Tropical Pacific Observed with GEOSAT	637
Ryuichi Kawamura: Intraseasonal and Interannual Modes of Atmosphere-Ocean System Over the Tropical Western Pacific	649
David Gutzler, and Tamara M. Wood: Observed Structure of Convective Anomalies	659
Siri Jodha Khalsa: Remote Sensing of Atmospheric Thermodynamics in the Tropics	665
Bingrong Xu: Some Features of the Western Tropical Pacific: Surface Wind Field and its Influence on the Upper Ocean Thermal Structure	677
Bret A. Mullan: Influence of Southern Oscillation on New Zealand Weather	687
Kenneth S. Gage, Ben Basley, Warner Ecklund, D.A. Carter, and John R. McAfee: Wind Profiler Related Research in the Tropical Pacific	699
John Joseph Bates: Signature of a West Wind Convective Event in SSM/I Data	711
David S. Gutzler: Seasonal and Interannual Variability of the Madden-Julian Oscillation	723
Marie-Hélène Radenac: Fine Structure Variability in the Equatorial Western Pacific Ocean	735
George C. Reid, Kenneth S. Gage, and John R. McAfee: The Climatology of the Western Tropical Pacific: Analysis of the Radiosonde Data Base	741

Chung-Hsiung Sui, and Ka-Ming Lau: Multi-Scale Processes in the Equatorial Western Pacific	747
Stephen E. Zebiak: Diagnostic Studies of Pacific Surface Winds	757

MISCELLANEOUS

Rick J. Bailey, Helene E. Phillips, and Gary Meyers: Relevance to TOGA of Systematic XBT Errors	775
Jean Blanchot, Robert Le Borgne, Aubert Le Bouteiller, and Martine Rodier: ENSO Events and Consequences on Nutrient, Planktonic Biomass, and Production in the Western Tropical Pacific Ocean	785
Yves Dandonneau: Abnormal Bloom of Phytoplankton around 10°N in the Western Pacific during the 1982-83 ENSO	791
Cécile Dupouy: Sea Surface Chlorophyll Concentration in the South Western Tropical Pacific, as seen from NIMBUS Coastal Zone Color Scanner from 1979 to 1984 (New Caledonia and Vanuatu)	803
Michael Szabados, and Darren Wright: Field Evaluation of Real-Time XBT Systems	811
Pierre Rual: For a Better XBT Bathy-Message: Onboard Quality Control, plus a New Data Reduction Method	823